Computational modelling of musculoskeletal to predict the human response with exoskeleton suit

Govinda Anantha Padmanabha

School of Mechanical Building and Sciences,
Vellore Institute of Technology (VIT) University,
Chennai, India
Email: govinda.a1990@gmail.com

Shravan Tata Ramalingasetty

Department of Aerospace Engineering,
Indian Institute of Science (IISc),
Bangalore, India
Email: shravantr@gmail.com

Boobalan Vetrivel

CSM software Pvt. Ltd.,
Bangalore, India
Email: boobalanvn@gmail.com

Indrajit Mukherjee and S.N. Omkar*

Department of Aerospace Engineering,
Indian Institute of Science (IISc),
Bangalore, India
Email: inder@aero.iisc.ernet.in
Email: omkar@aero.iisc.ernet.in
*Corresponding author

R. Sivakumar

School of Mechanical Building and Sciences,
Vellore Institute of Technology (VIT) University,
Chennai, India
Email: Sivakumar.r@vit.ac.in

Abstract: Wearable exoskeleton is an assistive device for humans to carry heavy loads over long distance. The main aim of the study is to analyse the effect of an exoskeleton on human body during stand to sit motion, the study is accomplished by the use of a biomechanical analysis software called LifeMOD®. In this work, the activations of biceps femoris, rectus femorus and tensor fasclae latae (TLF) have been studied. The muscle activations during stand to sit with exoskeleton is found to be lesser than normal human movement, resulting in reduced expenditure of human energy. The results are helpful in training the control algorithms that are dependent on muscle activations measured by surface electromyography and to establish a framework for the study of behaviour of muscle activation while performing various activities driven by wearable exoskeleton.

Keywords: muscle activation; LifeMod®; ADAMS®; Lagrangian dynamics; motion capture.

Reference to this paper should be made as follows: Padmanabha, G.A., Ramalingasetty, S.T., Vetrivel, B., Mukherjee, I., Omkar, S.N. and Sivakumar, R. (2020) 'Computational modelling of musculoskeletal to predict the human response with exoskeleton suit', *Int. J. Biomechatronics and Biomedical Robotics*, Vol. 3, No. 4, pp.169–181.

Biographical notes: Govinda Anantha Padmanabha was a graduate student in the School of Mechanical and Building Sciences at the VIT University, Chennai Campus. His research interests revolve around the design optimisation of generic configurations using high fidelity computational fluid dynamics (CFD) computations, optimisation algorithms with the assistance of surrogate modelling.

Shravan Tata Ramalingasetty worked as a Junior Research Fellow under the guidance of Dr. S.N. Omkar in the Department of Aerospace Engineering, Indian Institute of Science. He completed his Bachelors of Engineering in Mechatronics from the Manipal Institute of Technology. His areas of interests include bio-robotics, bio-mechatronics, and controls systems.

Boobalan Vetrivel is an Application Engineer at the Multibody Dynamic Simulation Team, CSM Software Private Limited, Bangalore, India. His research interest include biomechanics, computational mechanics, MBD simulation and prosthetic.

Indrajit Mukherjee is a PhD student in the Department of Aerospace Engineering, Indian Institute of Science since 2008. Prior to that, he obtained his Master in Structural Engineering, Department of Civil Engineering, IISc. He holds a Bachelor in Mechanical Engineering from the PESIT, Bangalore. His doctoral research involves exploring the aerodynamics and aeroelasticity of flapping wing-based micro aerial vehicles. Besides, his research interests are also in the areas of structural dynamics, nonlinear systems and stability analysis of dynamical systems.

S.N. Omkar is the Chief Research Scientist at the Department of Aerospace Engineering, Indian Institute of Science, Bangalore, India. His research interests include yoga, biomechanics, nature inspired computational techniques, satellite image processing and parallel computing.

R. Sivakumar is a Professor in the School of Mechanical and Building Sciences at the VIT University, Chennai Campus. His research interests include computational fluid dynamics, combustion, combustion instability and aero-acoustics.

1 Introduction

Demand to push the limits of physical capabilities of man is rising with the advancement of science and technology. It may be to help the physically disabled or to enhance the existing physical capabilities. One such technology is an external powered suit that attaches to a human body. When worn, it provides the additional strength and ability to achieve tasks that are not humanly possible or to perform tasks that are not possible due to certain disabilities. Such an external body suit is known as a wearable robot or more commonly called as exoskeleton. Exo means outside and skeleton implies support structure for strength. The concept of an external support frame for strength and protection has been inspired by nature (Guizzo and Goldstein, 2005). Examples of exoskeleton animals include insects such as grasshoppers and cockroaches, and crustaceans such as crabs and lobsters. Wearable exoskeletons have the ability to provide power to the wearer unlike the passive exoskeletons of animals in nature. Wearable exoskeletons find immense applications in military and rehabilitation purposes (Guizzo and Goldstein, 2005).

Academic research on exoskeletons for humans began as early as 1960 (Hong et al., 2013; Li at al., 2015). Guizzo and Goldstein (2005) discussed the development of exoskeletons from their inception and the activities of the leading research teams across the world in this field. Human wearable exoskeleton is an electro-mechanical device (Cenciarini and Dollar, 2011). It makes use of mechanical and electrical technologies to provide the benefits to wearers (Gams et al., 2013). Developing an exoskeleton involves multiple disciplines, the most important parts of any basic exoskeleton are: structure, actuators, sensors and controller. For smooth performance, all of the above have to work in synchronisation.

Extensive researches have been conducted on the development of exoskeletons to provide a better man-machine interface (Rahman et al., 2011; Zhang and Anderson, 2012). Zoss et al. (2005) and Kim et al. (2013) designed optimised structures for better end user comfort and efficient power transfer to the human body. Wang et al. (2011) and Onen et al. (2013) employed different types of actuators to meet the required torques and Kazerooni et al. (2005) developed intelligent control algorithms that work on the information acquired by multiple sensors. Hussain et al. (2013a) have shown how controlled robot extensions used for gait rehabilitation. The outcome of such studies can only be tested by building the actual model, and then experimenting it with the subjects for further feedback and improvements (Zoss and Kazerooni, 2005).

Building an exoskeleton poses two problems:

1 The exoskeletons are worn by human subjects. This imposes a high factor of risk. As discussed earlier, exoskeleton is a combination of multiple disciplines that need to work in harmony. A small glitch in any of the systems can lead to fatal injuries to human body. Thus, the system needs to be highly fault tolerant.

2 It is time consuming and an expensive way of evaluating the performance of a design.

The solution is to develop an environment to simulate the performance and interaction of the exoskeleton with the human body. This way one can ensure that the torques

imposed by the exoskeleton are well within the safety limits. The internal effects on the human body due to exoskeleton can be analysed safely. Any changes can be incorporated quickly to re-test for better performance results. The added advantage of such simulation is that we can compute muscle activations during activities. The muscle activation is an important parameter to analyse the performance of exoskeleton aiding human movements and the activation patterns are important in training control algorithms that make use of electromyography (EMG) sensors to predict human movements.

Cho et al. (2012) have adopted a similar approach for the above mentioned problem. They have utilised a bio-mechanics modelling software called AnyBody®, for studying the effect of exoskeleton on human body while lifting different weights. The torques are then measured at various human body joints with and without exoskeleton. However, the study did not focus on the individual muscles forces and activations. They also did not provide any mathematical validation of the results obtained. To capture the motion, they used optical vicon® system, which puts a restriction on place to capture motion. The above discussed points are tackled in this work. For the evaluation, a simple motion such as stand-to-sit task is chosen and simulated. Hussain et al. (2013b) simulated human robot interaction for cadence study using mathematical models under simplified conditions. However, this approach is not flexible for use in different studies.

In daily life, one of the most important and demanding activity performed several times a day is stand to sit motion (Tsukahara et al., 2010). The simultaneous extension of hip joint and ankle joint along with flexion of knee joint results in sitting down motion. Hip joint flexion requires actuation of muscles of fasciae latae (TFL) and rectus femoris whereas knee joint flexion requires actuation of muscle of biceps femoris (BiFEM) (He et al., 2007). In fact, for the purposes of rehabilitation in cases of injury to spinal cord, cerebrovascular region, etc., stand to sit training is highly emphasised by medical doctors and physical therapists (Tsukahara et al., 2010). The expenditure of human energy during manoeuvring from stand to sit is reduced with the help of an exoskeleton.

The effect of exoskeleton on human body during stand to sit motion can be analysed by using a biomechanics modelling software. LifeMOD®, a plug-in to ADAMS® (multibody dynamics software), developed by Life Modeler Inc. It can generate a three dimensional computer model of human body. LifeMOD® software has been used in studies in the fields of medical, sports and exercise (Boobalan et al., 2014; De Jongh, 2007; Hofmann et al., 2006; Nolte et al., 2013). The analysis of stand to sit of human body and exoskeleton can be done using a combination of LifeMOD® and ADAMS®. ADAMS® can be employed to build a 'virtual machine' of a complex mechanical system. Nolte et al. (2013) have described that the interaction between musculoskeletal human body and mechanical systems can be simulated using LifeMOD®.

Zhu et al. (2015) studied the effect of exoskeleton on human body while walking using LifeMOD® software. The lower extremity joint torques namely, hip, knee and ankle joint torques were computed with and without exoskeleton. However, their study did not provide any mathematical validation of the results obtained.

Primary requirement to accomplish this task is to design an exoskeleton based on conventional mechanical modelling techniques. A simple six DOF lower extremity exoskeleton is designed using SolidWorks®. The next step is to export the model into LifeMod® environment for simulations. The final step is to capture the real human motion; inertial sensors are used over camera-based motion capture techniques. Inertial measurement units (IMUs) prove to be very suitable to realise indoor and outdoor applications because of their immense portability, compactness and useful, accurate movement information they supply (Mayagoitia et al., 2002; Zhu and Zhou, 2004). The angular measurements are saved with respective time stamps and the data is exported to the simulation environment at the respective segments.

The captured motion is used to simulate the stand to sit motion both with and without exoskeleton. A mathematical model based on Lagrangian dynamics is developed to validate the joint torques obtained from the simulation of stand to sit motion without exoskeleton in LifeMOD®. For mathematical simplicity, the human joints modelled are assumed to be ideal with no joint stiffness and damping (Music et al., 2008). The sit to stand motion is symmetric with respect to sagittal plane (Lundin et al., 1995), as stand to sit being the opposite of sit to stand, the same assumption is valid and this makes it possible to project the results obtained by carrying out the measurements on only one side of the body and also applicable to the other side as well. The torques computed from the mathematical model and the software are validated. The validation allows us to then change the mathematical model to include the exoskeleton and compute torques from it. The calculated torques act as the actuator drive elements to move the exoskeleton attached to the body.

The training and simulation of human body to perform the task is described in the methodology section. The simulated motion of both the cases, without and with exoskeleton provides a large amount of information on different parameters of the human body. The parameters of interest are the joint torques, joint angular rates and the most important of all the activation pattern of various muscles involved in the motion. In this paper, the discussed framework provides a platform to simulate various types of exoskeleton models performing real life movements.

2 Methodology

The paper deals with evaluation of muscle activity of a subject driven by an exoskeleton during stand to sit motion. Thus section deals with design of exoskeleton, capture of stand to sit motion, mathematical modelling and simulation of the performance.

2.1 Exoskeleton structure

Exoskeleton mainly consists of two parts, namely upper extremity exoskeleton and lower extremity exoskeleton (Cenciarini and Dollar, 2011). This paper focuses on lower extremity exoskeleton as it contributes significantly during stand to sit motion. A simple exoskeleton structure is designed as this paper focuses only on the biomechanical aspect. The design of the exoskeleton structure (Figure 1) should support the payload and provide the mechanical interface with the operator. The mechanical design consists of designing foot, shank, thigh and torso. The dimensions required for the exoskeleton design has been calculated by considering the total load (Exoskeleton weight + human weight) using DATA Handbook (Lingaiah, 2006) (Table 1).

Table 1 Dimensions of exoskeleton

Sl. no.	*Parts*	*Dimensions (mm)*
1	Foot	355.6
2	Shank link	330 (length), 30 (outer diameter), 15 (inner diameter)
3	Thigh link	380 (length), 30 (outer diameter), 15 (inner diameter)
4	Hip	220 (width), 220 (depth), 30 (outer diameter), 15 (inner diameter)

Table 2 Exoskeleton's DOF

Joint	*Degree of freedom (DOF)*	*Description*
Ankle	1	Flexion/extension
Knee	1	Flexion
Hip	1	Flexion/extension

Figure 1 Exoskeleton structure (see online version for colours)

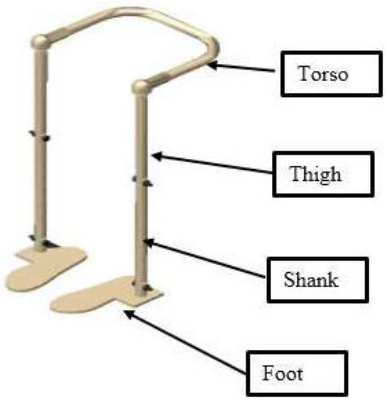

The cross-section of the thigh, shank and torso links are circular in shape as it has the advantages of lightness and high area moment of inertia when compared to other cross-sectional shapes in all the directions (Kim et al., 2013). The design consists of six degree of freedom (DOF): Each leg of the exoskeleton consists of 3 DOFs with 1 DOF at hip, 1 DOF at knee and 1 DOF at ankle (Table 2).

2.2 Motion capture

For both mathematical modelling and simulation, subject's motion has to be recorded. This involves recording of angular displacements and linear displacements, but the chosen movement involves only angular movement. IMU's have immense portability, compactness and can supply information that is useful and accurate. These characteristics of IMUs make them highly congruous for outdoor applications. An IMU is an electronic device that measures and reports angular velocity, orientation and gravitational forces, using a combination of accelerometers and gyroscopes, sometimes also magnetometers. IMU used for the experiment consists of a three axis accelerometer (± 8 g), a three axis gyroscope (± 2,000 degree/sec) and a three axis magnetometer ± 8 g). The IMU is from X-IMU®, the sensor has been calibrated by the manufacturer to obtain reliable readings for scientific purposes (Figure 2). The data from the three sensors are sampled at 128 Hz and the MARG algorithm running on the on-board microcontroller fuses the data from the three different sensors to obtain accurate angular rotation. The IMU's are strapped on to the subject using a special Velcro strap provided with an IMU holder, this ensures a firm placement of the sensor onto the body. The data is transferred to a nearby computer using USB data cable. The angular measurements are saved on to an excel sheet with respective time stamps. The time stamps are used to synchronise the time of the three IMU's.

Figure 2 Inertial measurement unit (see online version for colours)

2.3 Experimental protocol

The test consisted of one individual (male, aged 22 years, weight 60 kg, height 186 cm). The subject is healthy, without any problems in the musculoskeletal system. For positioning of IMU's: Shank length is measured from 0.5 cm anterior to the visually determined approximate knee centre of rotation, thigh length is measured from the knee centre of rotation to the great trochanter and trunk length from the greater trochanter to the centre of shoulder glenohumeral rotation measured in the neutral position. Segment lengths, mass of the segments and the CG position for the subject is taken from the anthropometric data (Figure 3).

Figure 3 Measurement setup (see online version for colours)

Notes: (1) HAT inertial sensing unit, (2) thigh inertial sensing unit, (3) shank inertial sensing unit, (4) seat.

2.4 Mathematical modelling

In this section, we enumerate the development of the mathematical model for the human body. The motion of a three segment human body model in sagittal plane with three DOF can be employed to estimate the motion of a human body involved in the transition from a standing stance to sitting. As a result, a three DOF model, comprising of three segments namely HAT, thigh and shank. The model is used to validate the torques developed at the joints as torques cannot be directly measured from the sensors mounted at the joints. A schematic diagram of the model is shown in Figure 4. The parameters θ_1, θ_2 and θ_3 denote the angular positions, I_{x_1}, I_{x_2} and I_{x_3} denote segment moment of inertia, l_1, l_2 and l_3 represent segment length and l_{c_1}, l_{c_2} and l_{c_3} represent position of segment centre of mass with respect to distal joint, at HAT, thigh and shank respectively; with respect to the horizontal plane. Anthropometric data is used to establish segment masses, lengths, moments of inertia and CoM positions (Table 3).

Table 3 Subject data for mathematical modelling

Parameters	*Link1*	*Link2*	*Link3*
Mass (kg)	5	8	50
Length (mm)	380	371	980
CG length (mm)	196	172	351.5

Using the kinematic variables mentioned above, the expression for kinetic energy T can be obtained as

$$T = \sum_{i=1}^{n=3} T_i$$

where T represents the total kinetic energy and T_i denotes the kinetic energy of the segment i. T_i's can be stated as

$$T_1 = \frac{1}{2} I_{x_1} \dot{\theta}_1^2 + \frac{1}{2} m_1 \left[\dot{\theta}_1^2 l_{c_1}^2 \right]$$

$$T_2 = \frac{1}{2} I_{x_2} \dot{\theta}_2^2 + \frac{1}{2} m_2 \left[\dot{\theta}_1^2 l_1^2 + \dot{\theta}_2^2 l_{c_2}^2 \right] + 2\left[\dot{\theta}_1 \dot{\theta}_2 l_1 l_{c_2} \cos(\theta_1 - \theta_2) \right]$$

$$T_3 = \frac{1}{2} I_{x_3} \dot{\theta}_3^2 + \frac{1}{2} m_3 \left[\dot{\theta}_1^2 l_1^2 + \dot{\theta}_2^2 l_2^2 + \dot{\theta}_3^2 l_{c_3}^2 \right] + 2\left[\dot{\theta}_1 \dot{\theta}_2 l_1 l_2 \cos(\theta_1 - \theta_2) + \dot{\theta}_2 \dot{\theta}_3 l_2 l_{c_3} \cos(\theta_2 - \theta_3) + \dot{\theta}_1 \dot{\theta}_3 l_1 l_{c_3} \cos(\theta_1 - \theta_3) \right]$$

where $\dot{\theta}_1$, $\dot{\theta}_2$, $\dot{\theta}_3$ is the angular velocity at HAT, thigh and shank segment, respectively. Similarly, the expression for the potential energy V can be stated as

$$V = \sum_{i=1}^{n=3} V_i$$

where V_i denotes the kinetic energy of the segment i and V represents the total potential energy. V_i's can be expressed as

$$V_1 = m_1 g h_1 = m_1 g l_{c_1} \sin\theta_1$$

$$V_2 = m_2 g h_2 = m_2 g \left[l_1 \sin\theta_1 + l_{c_2} \sin\theta_2 \right]$$

$$V_3 = m_3 g h_3 = m_3 g \left[l_1 \sin\theta_1 + l_2 \sin\theta_2 + l_{c_3} \sin\theta_3 \right]$$

Figure 4 Notation of three segment human body model parameters

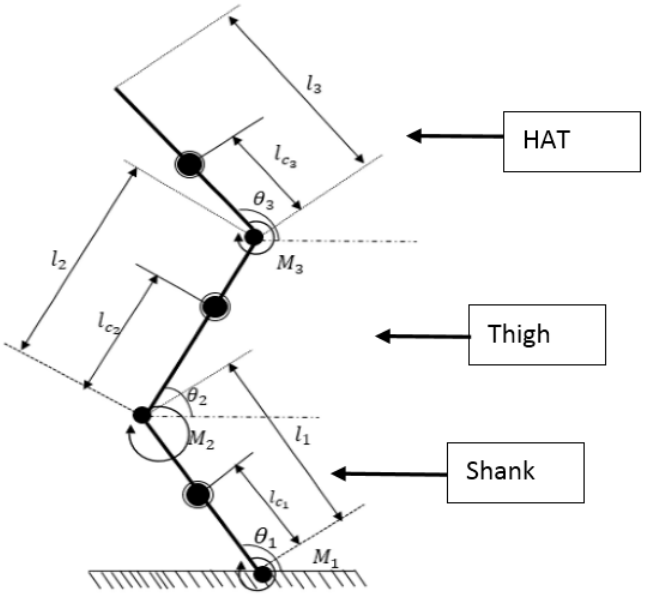

From the kinetic and potential energy expressions, we proceed to obtain the Lagrangian as follows:

$$L = T - V$$

On simplification, we have

$$\begin{aligned} L = {} & \frac{1}{2} I_{x_1} \left[\dot{\theta}_1^2 + \dot{\theta}_2^2 + \dot{\theta}_3^2 \right] + \frac{1}{2} \left(m_1 \dot{\theta}_1^2 l_{c_1}^2 \right) \\ & + m_2 \left[\dot{\theta}_1^2 l_1^2 + \dot{\theta}_2^2 l_{c_2}^2 + +2\dot{\theta}_1 \dot{\theta}_2 l_1 l_{c_2} \cos(\theta_1 - \theta_2) \right. \\ & + m_3 \left[\dot{\theta}_1^2 l_1^2 + \dot{\theta}_2^2 l_2^2 + \dot{\theta}_3^2 l_{c_3}^2 \right] \\ & + 2 \left[\dot{\theta}_1 \dot{\theta}_2 l_1 l_2 \cos(\theta_1 - \theta_2) \right. \\ & + \dot{\theta}_2 \dot{\theta}_3 l_2 l_{c_3} \cos(\theta_2 - \theta_3) \\ & \left. \left. + \dot{\theta}_1 \dot{\theta}_3 l_1 l_{c_3} \cos(\theta_1 - \theta_3) \right] \right] \end{aligned}$$

The governing equation of motion for multi-segmental system is derived using the Lagrange's equation:

$$\frac{d}{dt}\left(\frac{\partial L}{\partial \dot{\theta}_i} \right) - \frac{\partial L}{\partial \theta_i} = Q_i$$

The governing equation of motions of the different segments can be obtained as follows.

For HAT,

$$\begin{aligned} & \frac{d}{dt}\left(\frac{\partial L}{\partial \dot{\theta}_3} \right) - \frac{\partial L}{\partial \theta_3} = \left[\ddot{\theta}_3 \left(m_3 l_{c_3}^2 + I_{x_3} \right) \right. \\ & + \ddot{\theta}_1 m_3 l_1 l_{c_3} \cos(\theta_1 - \theta_3) + \ddot{\theta}_2 m_3 l_2 l_{c_3} \cos(\theta_2 - \theta_3) \\ & - \dot{\theta}_1^2 m_3 l_1 l_3 \sin(\theta_1 - \theta_3) - \dot{\theta}_2^2 m_3 l_2 l_3 \sin(\theta_2 - \theta_3) \\ & \left. + g m_3 l_{c_3} \cos\theta_3 \right] = M_3 \end{aligned}$$

$$\begin{aligned} & \frac{d}{dt}\left(\frac{\partial L}{\partial \dot{\theta}_2} \right) - \frac{\partial L}{\partial \theta_2} = \left[\ddot{\theta}_2 \left(m_3 l_2^2 + m_2 l_{c_2}^2 + I_{x_2} \right) \right. \\ & + \ddot{\theta}_1 \left(m_3 l_1 l_{c_2} + m_3 l_1 l_2 \right) \cos(\theta_1 - \theta_2) \\ & + \ddot{\theta}_3 m_3 l_2 l_{c_3} \cos(\theta_2 - \theta_3) - \dot{\theta}_1^2 \left(m_3 l_1 l_2 + m_3 l_1 l_{c_2} \right) \sin(\theta_1 - \theta_2) \\ & - \dot{\theta}_3^2 m_3 l_2 l_{c_3} \sin(\theta_2 - \theta_3) \\ & \left. + g \left(m_2 l_{c_2} + m_3 l_2 \right) \cos\theta_2 \right] = M_2 - M_3 \end{aligned}$$

$$\begin{aligned} & \frac{d}{dt}\left(\frac{\partial L}{\partial \dot{\theta}_1} \right) - \frac{\partial L}{\partial \theta_1} = \left[\ddot{\theta}_1 \left(m_3 l_2^2 + m_2 l_1^2 + m_1 l_{c_1}^2 + I_{x_1} \right) \right. \\ & + \ddot{\theta}_2 \left(m_2 l_1 l_{c_2} + m_3 l_1 l_2 \right) \cos(\theta_1 - \theta_2) \\ & + \ddot{\theta}_3 m_3 l_2 l_{c_3} \cos(\theta_2 - \theta_3) \\ & - \dot{\theta}_2^2 \left(m_3 l_1 l_2 + m_3 l_1 l_{c_2} \right) \sin(\theta_1 - \theta_2) \\ & - \dot{\theta}_3^2 m_3 l_1 l_{c_3} \sin(\theta_1 - \theta_3) \\ & \left. + g \left(m_1 l_{c_1} m_2 l_1 + m_3 l_2 \right) \cos\theta_1 \right] = M_1 - M_2 \end{aligned}$$

2.5 Simulation

As discussed earlier, LifeMOD® developed by Life Modeler Inc. is a three-dimensional computer model of human body which can be modified by changing the anthropometric data of the subject required such as age, gender, height, weight, etc. The established human body model can be combined with the physical environment for dynamic interaction. The outputs of the simulation can be contact force, angular orientation, angular velocity, acceleration and joint torques and muscle activation. There are two types of models, namely the active model and the passive model. Passive model (i.e., dummy elements) is applied for studies of crash analysis. In this project, active model is used to study the human stand to sit manoeuvring. The development of the three-dimensional computer model of human body begins with the generation of body segments, joint stiffness, soft tissue and creating individual motion agents.

In this software, the body segments are represented as rigid bodies, this can be generated from the standard anthropometric database. In this work, GeBOD database of the subject is modelled and analysed. It can create a human body model according to the simple information, such as height, weight, age and gender. The body parameters of the created human body model can also be further modified by the user. After creating the human segment, the passive joint details are applied for the inverse dynamic analysis. The user-defined properties such as stiffness, damping, angular limits and limit stiffness can record the angulation patterns when the model is driven by the motion capture data in the inverse dynamics simulation. After that, the motion agent (i.e., motion capture data) is disabled, so that the trained muscles will drive the musculoskeletal in forward dynamics. The physical model of a chair is simulated as a single part on which the human body rest's while in sitting position.

Figure 5 LifeMOD® muscles system and position of motion agents (see online version for colours)

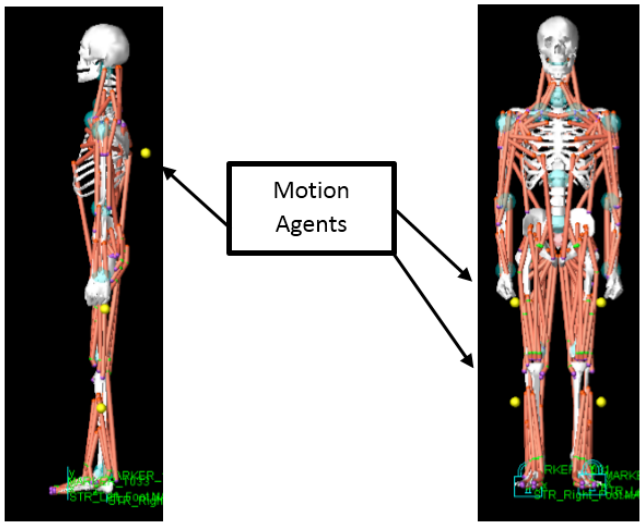

2.6 Integration with IMU data

The forward dynamics and inverse dynamics methods are applied during simulations. Inverse dynamics simulations are performed for human stand to sit with the help of the motion agents (Figure 5). During the inverse dynamics simulation, the angular orientation from various IMUs are applied with the help of the motion agents positioned on the centre of gravity of three segments viz., HAT, thigh and

shank (Figure 6). The data of the marker trajectories is applied to drive the motion agents. The muscles are trained during the inverse dynamics simulation in order to result in the required stand to sit movement. After the inverse dynamics simulation is performed, the motion agents are deactivated from the model. The muscle force is then used to drive the model during the forward dynamics simulation in the manner as developed through the inverse dynamics simulation (Figure 7). During the forward dynamics simulation, the model is guided by the internal forces (muscle-length changes resulting in joint angulations and torques) and influenced by external forces (gravity, contact and determined exercise resistance).

Figure 6 Stand to sit movement performed by the subject (see online version for colours)

Figure 7 Series of human simulation from time 0 to 4.08 sec (see online version for colours)

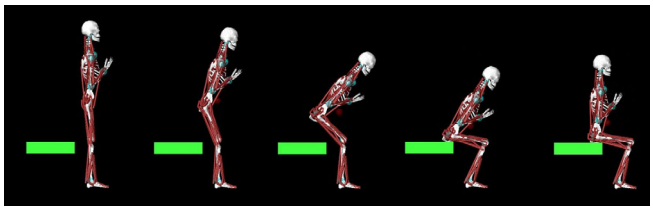

Figure 8 Series of exoskeleton simulation from time 0 to 4.08 sec (see online version for colours)

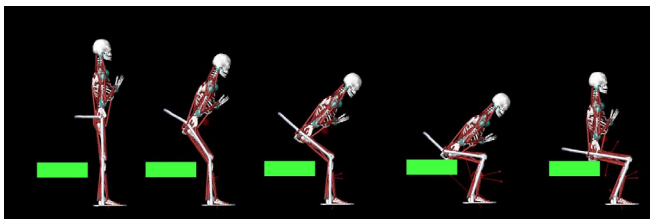

2.7 Exoskeleton

The forward dynamics methods are applied during the simulations. The joint torques obtained from the mathematical model is used to drive the exoskeleton during the forward dynamics simulation (Figure 8) in the manner as developed through the inverse dynamics simulation (Figure 5). Bushing joints are used to link hip, thigh and shank of the human body with exoskeleton model. Bushing elements make limited translational and rotational motion.

Further, altering of stiffness and damping characteristics make it possible to regulate the amount of motion in all three orthogonal directions. Hence bushing elements are chosen over fixed joint elements. Default joint parameters (stiffness $(K) =$10^4$$, dampening (C) = 1,000) define the original joints constituted in the bio-mechanical model. A comparatively 'rigid' model can result in a stable and smooth motion when manipulated by motion splines. Hence, joints having high joint stiffness are created. AKISPL (Akima-fitting method) is adopted to drive the human body. In MSC ADAMS, the AKISPL is a spline function that can be adopted for the huge experimental date to obtain smooth motion, which has been applied to the revolute joint between two links resulting in driving the human body to replicate the more realistic movement (Figure 9).

Figure 9 Measurement setup for exoskeleton stand to sit (see online version for colours)

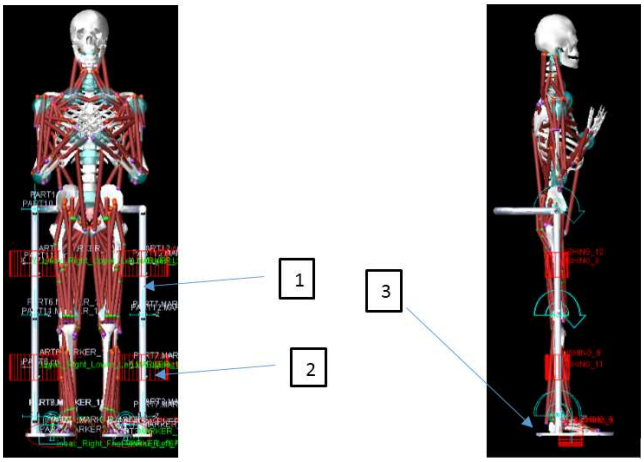

Notes: (1) Exoskeleton, (2) bushing and (3) revolute joint.

3 Results and discussion

This section deals with results of the analysis discussed in the methodology section. The flow of the section follows that of the methodology section. The initial graphs deal with the data of the performance for STS without exoskeleton and latter with exoskeleton. The motion captured in the sagittal plane using IMU's placed on the body segments are fed to the respective joint segments in LifeMOD®. After training the model to perform the STS task, the muscles drive the human body model in LifeMod® to perform the same action. In order to verify if indeed the same action is performed or not, the angular rates from the simulation is validated with that of the IMU readings.

Figure 10 shows the graphs for angles in degrees from IMU and LifeMOD® at HAT, shank and thigh segments. The correlation between the graphs shows that human model precisely mimics the angular positions for STS motion. Also a comparison is established between angular rates from IMU and LifeMod®. Figure 11 and Figure 12 show the angular velocity and angular accelerations at the respective joint segments. Even though the angles from IMU and LifeMOD® are almost same, the angular rates differ a little more from simulation to reality. The differences can probably be attributed to the mathematical

solvers in the software or to the flexible Velcro straps used for mounting of sensors on to the human body while performing the experiment. Both reasons can lead to variations in angular rates but the angular positions are highly accurate, which is of higher importance in the study.

Figure 10 Comparison of angular orientation obtained from IMU and LifeMOD® software (see online version for colours)

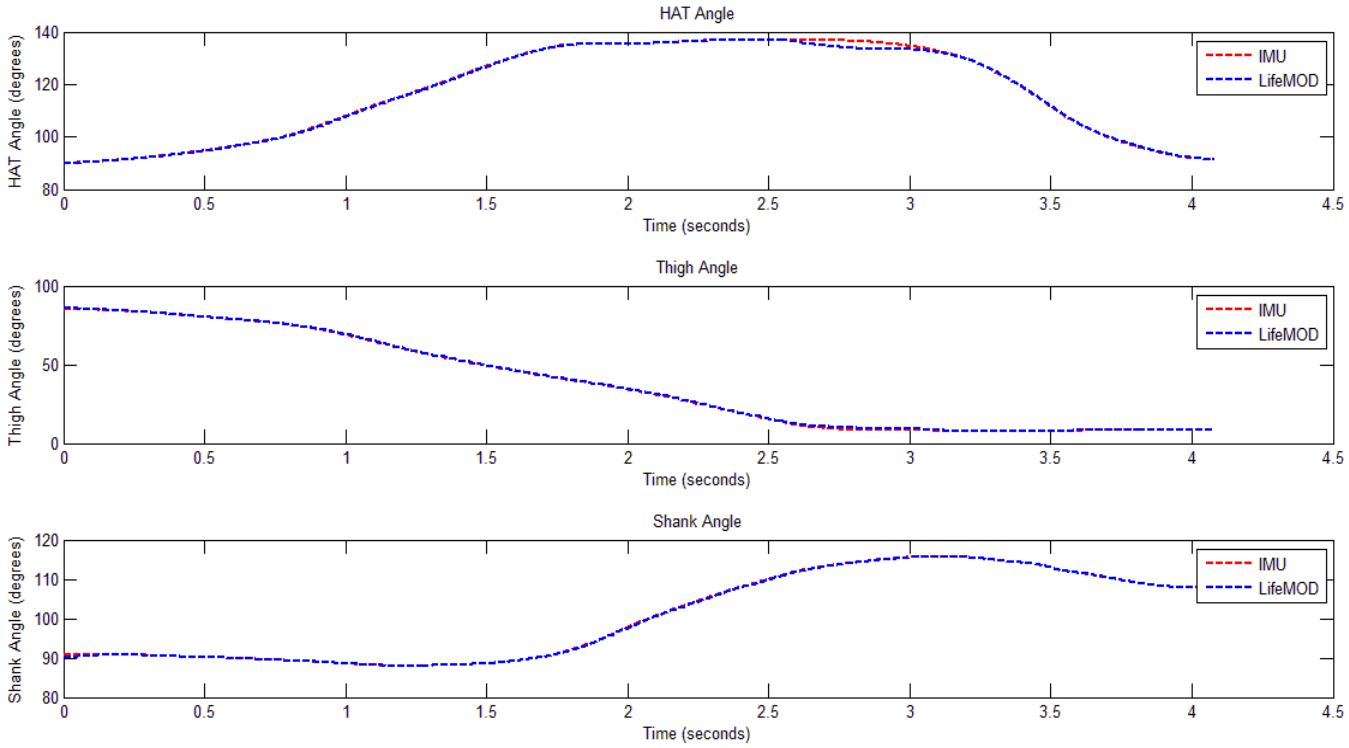

Figure 11 Comparison of angular velocity obtained from IMU and LifeMOD® software (see online version for colours)

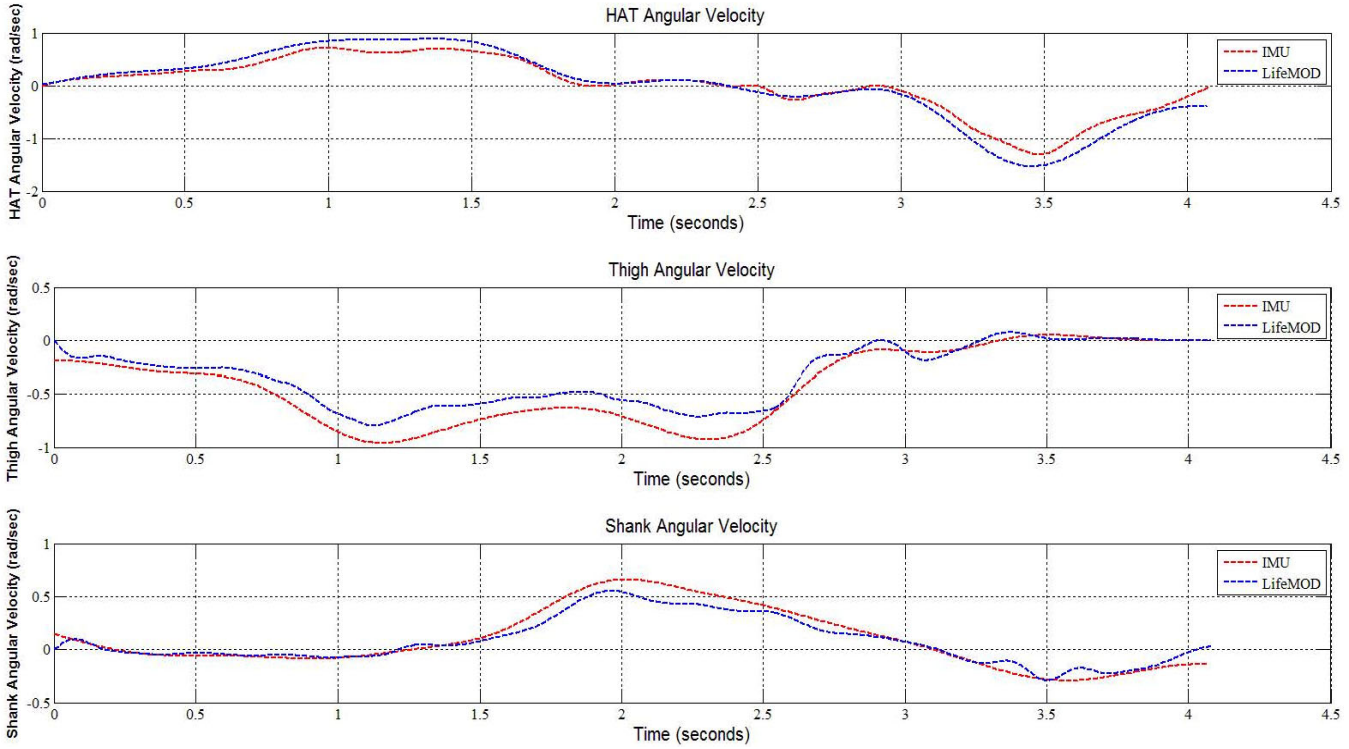

Figure 12 Comparison of angular acceleration obtained from IMU and LifeMOD® software (see online version for colours)

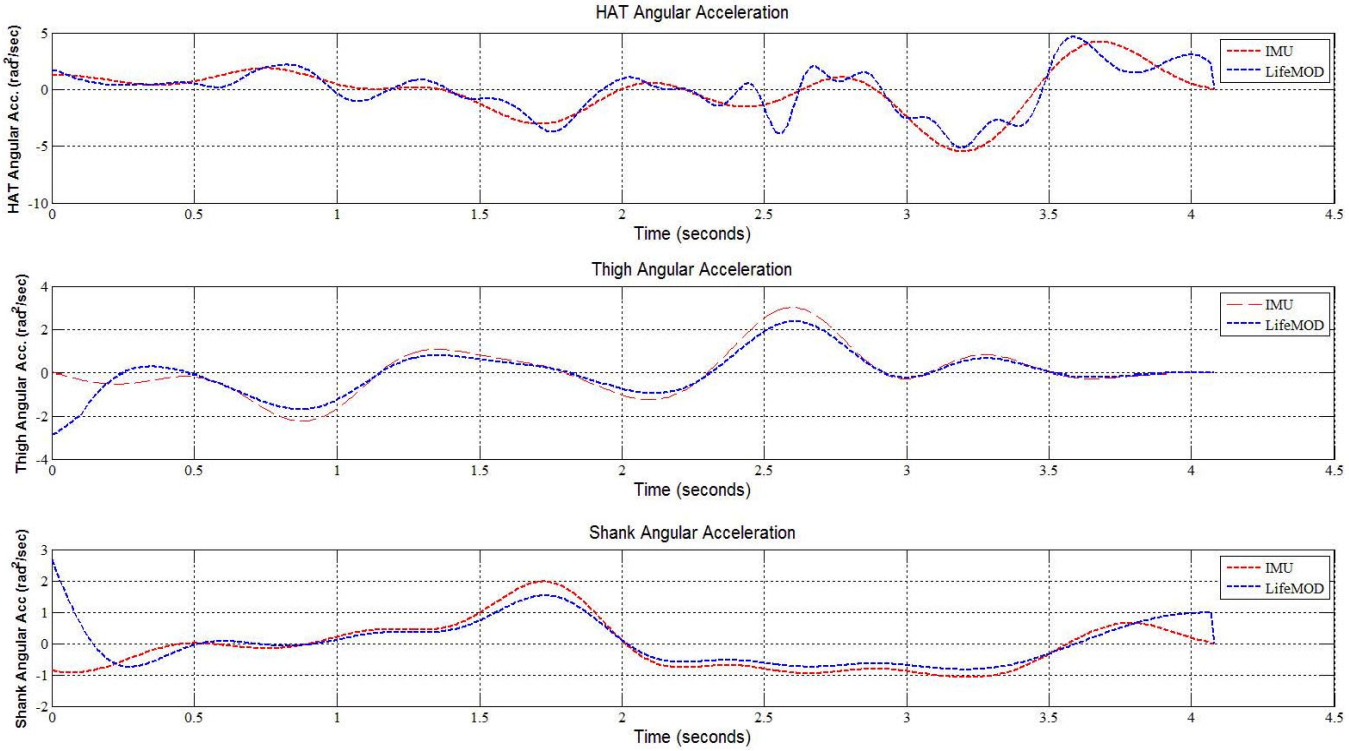

Figure 13 Comparison of torques obtained from IMU and LifeMOD® software (see online version for colours)

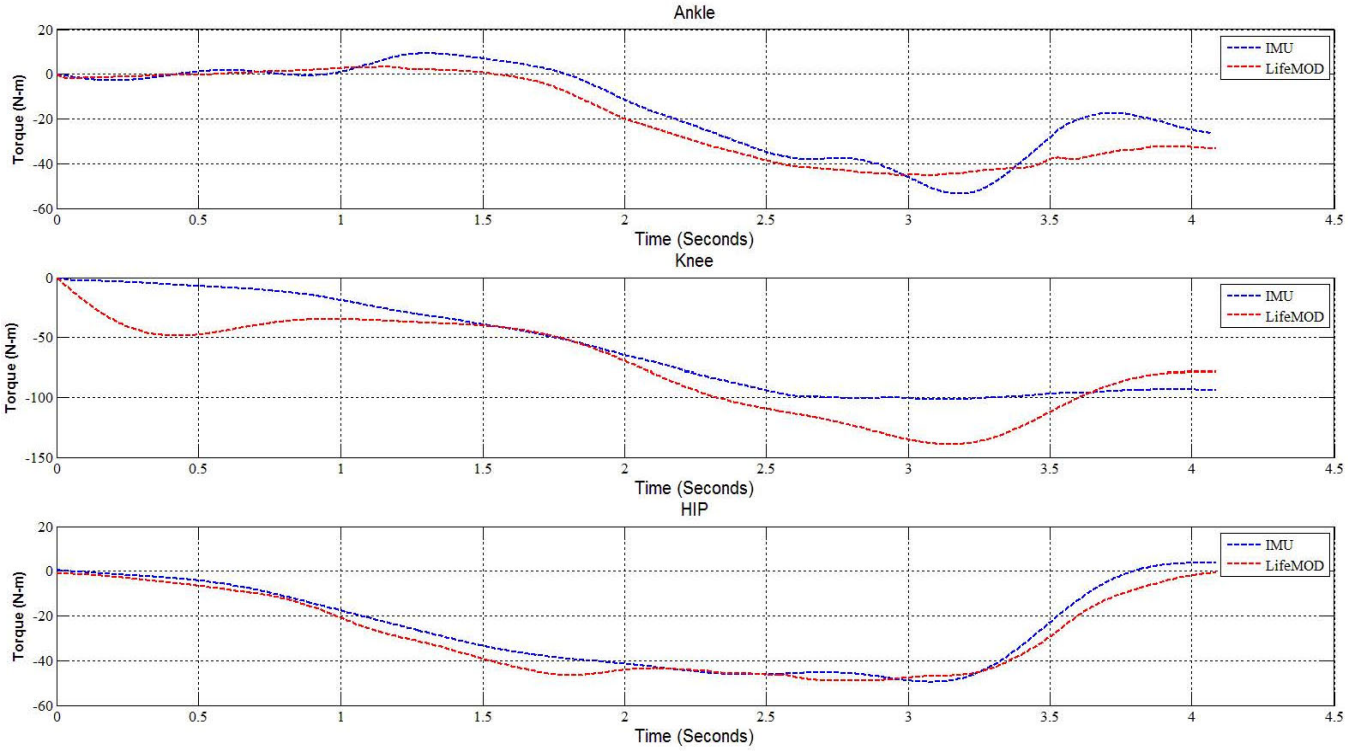

Figure 14 Torques required of drive the human body during the forward dynamics simulation (see online version for colours)

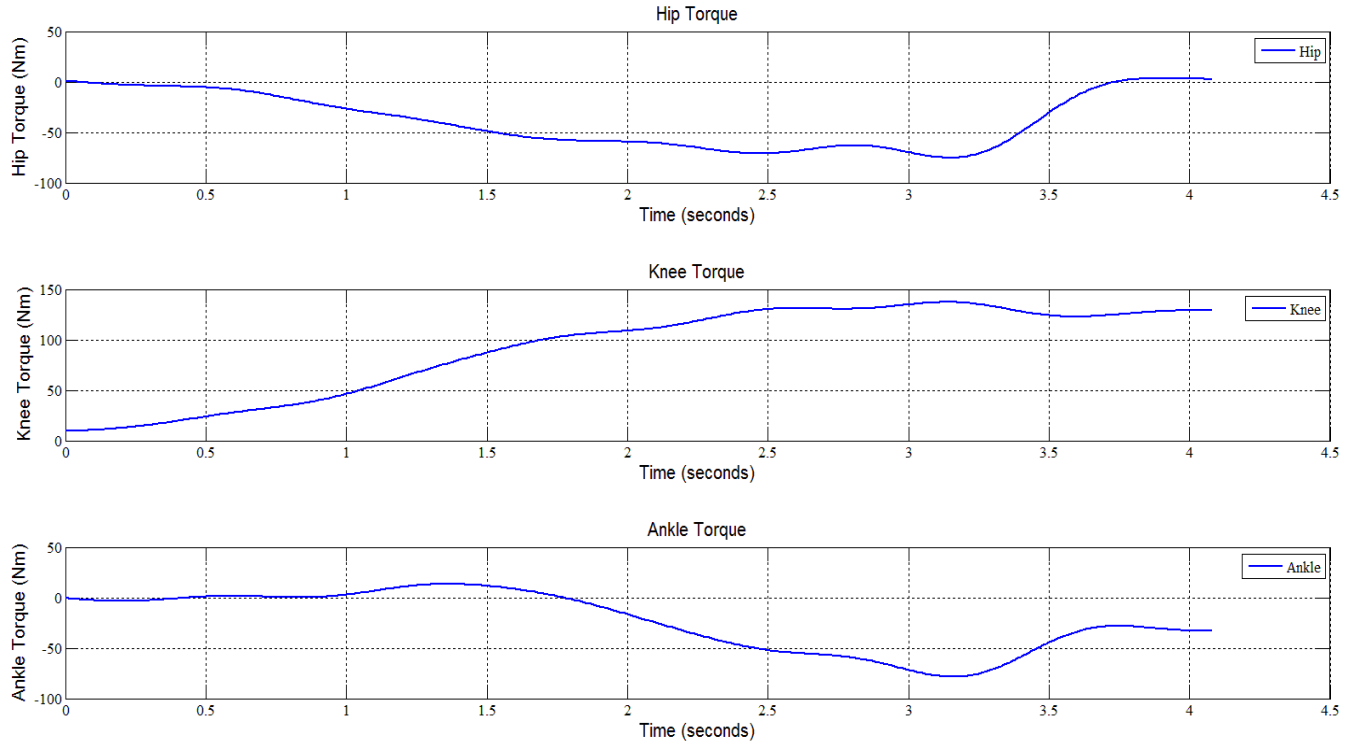

Figure 15 Comparison of segments angles obtained from IMU and LifeMOD® software after exoskeleton simulation (see online version for colours)

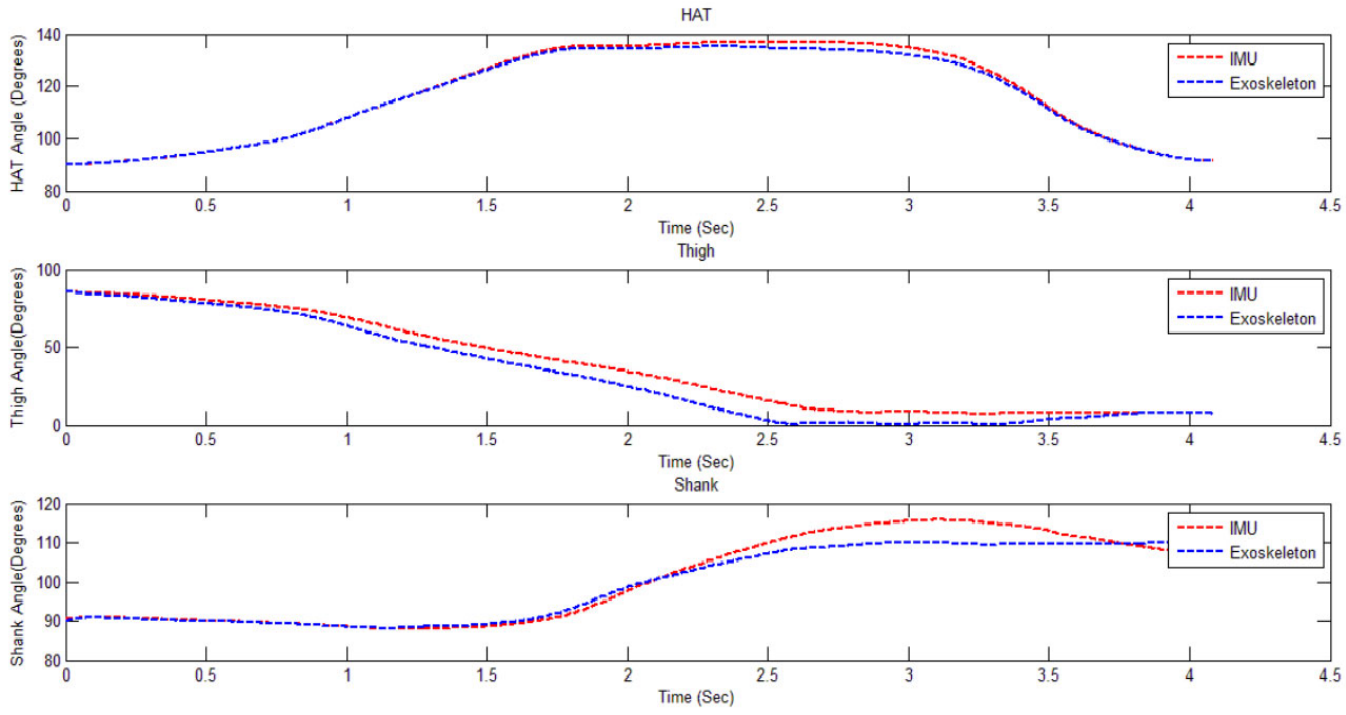

The mathematical model using Lagrangian dynamics is validated using the torque results obtained from the simulations. Figure 13 shows the torques obtained from angular rates of IMU for STS using Lagrangian modelling and LifeMOD® simulation. We can observe that even though the same IMU results are used for both math model and simulation, a difference in torque values are observed. In the mathematical modelling, for ease of modelling the joints are considered to be ideal but in LifeMOD® joint stiffness are provided. The pattern and the magnitudes of torques from mathematical Modelling are in close match to the torques obtained using LifeMOD®. The data is validated to make sure that the STS movement simulated is as close to the real captured performance as possible. Since the

simulation now represents the actual STS movement performed by the test subject, the muscle activations of the three major muscles discussed in the earlier sections can be plotted.

3.1 Exoskeleton

The next set of results correspond the analysis performed for STS using exoskeleton. Here, the exoskeleton drives the passive human body to which it is attached. To drive the exoskeleton and in turn make the human body perform the captured STS movement, joint torques have to be supplied to the six exoskeleton joints. The torques are computed using Lagrangian dynamics considering the exoskeleton model. Figure 14 represents the three joint torques at the hip, knee and ankle.

Figure 16 Muscle activation of human body during stand to sit (see online version for colours)

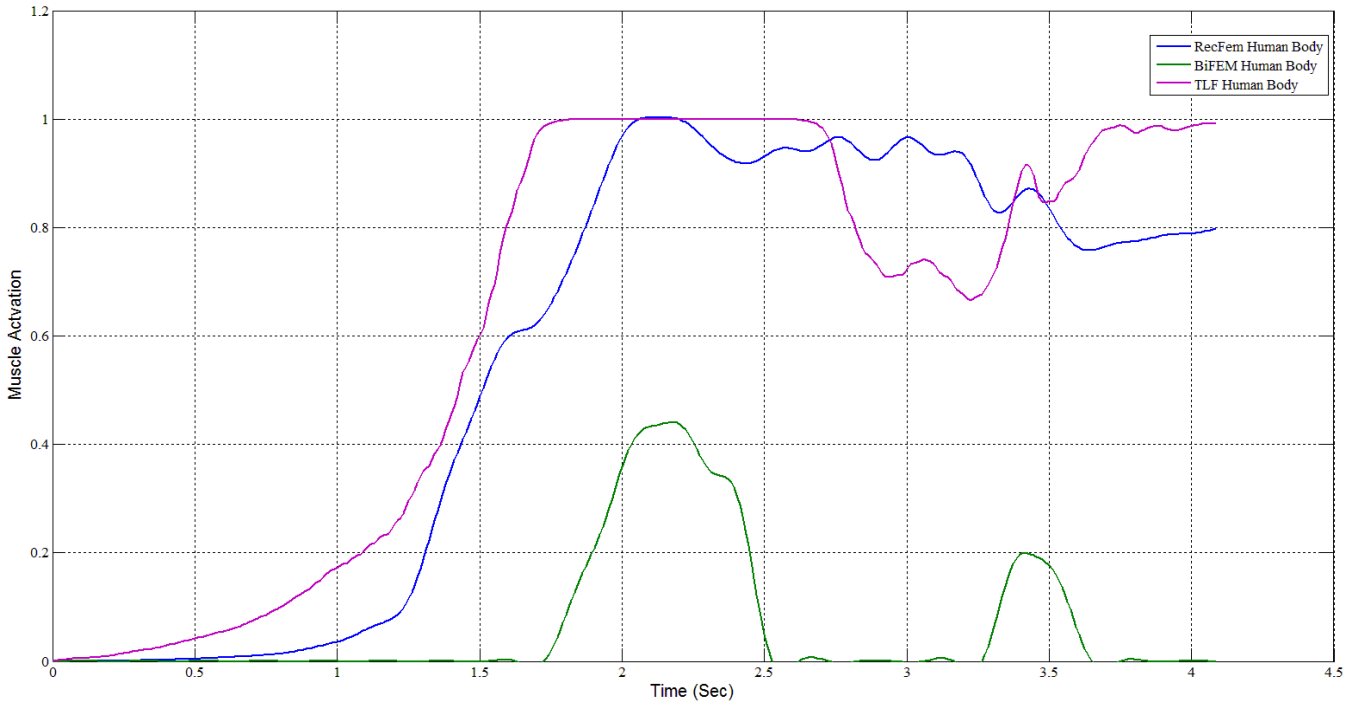

Figure 17 Muscle activation of human body stand to sit with exoskeleton (see online version for colours)

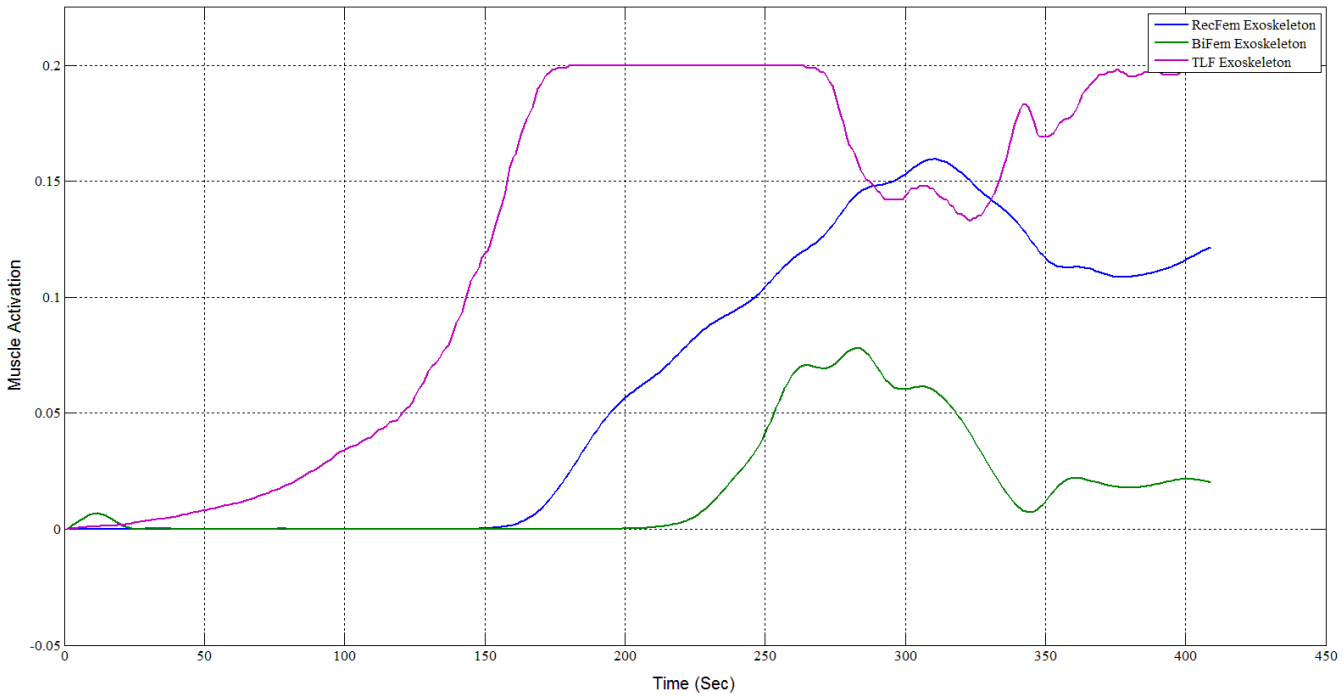

The simulation is carried out using the torques in Figure 14 to drive the exoskeleton. The obtained segment angles from the simulation are plotted against the segment angles obtained from IMU mounted on the subject performing STS. Figure 15 shows that the computed torques drove the exoskeleton to make the human body model perform STS same as the captured motion. The entire simulation is carried out without changing the anthropometric data.

3.2 Muscle activation

Muscle activations obtained from exoskeleton driven simulation are plotted against those obtained from computations without exoskeleton for the same set of three major muscles groups in Figure 16 and Figure 17. Figure 16 represents the muscle activation patterns of three muscles while the subject performs STS movement without an exoskeleton and Figure 17 represents the muscle activation patterns of three muscles while the subject performs STS movement with an exoskeleton. The activations are plotted versus time, and thus observations can be precisely made about when the peak activations occurred or the activation value at a particular pose during STS. The activations represented are normalised values, where 1 represents maximum activation and 0 represents minimum activation. From Figure 16 and Figure 17, it is evident that the muscle activation of biceps femoris (BiFEM), tensor fasciae latae (TFL) and rectus femoris (RecFem) muscles during human stand to sit maneuvering is found to be more when compared to exoskeleton stand to sit movement.

4 Conclusions and further work

This paper solely focuses on biomechanical aspects of human lower extremity during stand-to-sit motion, with and without Exoskeleton. The exoskeleton design has been validated using LifeMOD® software, to which real-time data obtained from IMUs is input. Torques computed using mathematical model (Lagrangian Dynamics) is compared to that obtained from LifeMOD® software and hence verified. This verification allows us to then change the mathematical model to include the exoskeleton and compute torques using it. The muscle activation during stand to sit with exoskeleton was found to be less when compared to that without exoskeleton, implying reduced expenditure of human energy during the latter. In this work, the stand to sit motion of human body is restricted to sagittal plane. Only three important muscles that are responsible for STS are considered. In addition, joints are considered to be ideal in the mathematical model for the purpose of simplicity. This work is confined to just stand to sit motion and muscle activation.

Further study can be done by considering several other muscles responsible for manoeuvring of human body and exoskeleton during STS, walking and STS motion. Analysed results can be used to design a control system for lower-limb exoskeleton and also establish a framework for studying of behaviour of muscle activation while performing various activities driven by wearable exoskeleton.

Acknowledgements

The first author expresses heartfelt thanks to Mr. S.K. Sachin, Research Intern, Department of Aerospace Engineering, Indian Institute of Science, Bangalore for his help in copy editing this paper. The authors would like to thank the reviewers for their comments which were useful during the revision of this study.

References

Boobalan, V., Omkar, S.N., Ramesh, D.V. and Shankar, S. (2014) 'Simulation of muscle activation patterns in the hip joint during normal level walking followed by sit-to-stand movement between two hip implants', *Trends Biomater. Artif. Organs*, Vol. 28, No. 1, pp.19–25.

Cenciarini, M. and Dollar, A.M. (2011) 'Biomechanical considerations in the design of lower limb exoskeletons', *IEEE International Conference on Rehabilitation Robotics*.

Cho, K., Kim, Y., Lee, D-y. and Lee, K. (2012) 'Analysis and evaluation of a combined human-exoskeleton model under two different constraint conditions', *International Summit on Human Simulation*, Florida, USA.

De Jongh, C. (2007) *Critical Evaluation of Predictive Modelling of a Cervical Disc Design*, Unpublished dissertation, University of Stellenbosch, Stellenbosch.

Gams, A., Petric, T., Debevec, T. and Babic, J. (2013) 'Effects of robotic knee-exoskeleton on human energy expenditure', *IEEE Transactions on J. Biomedical Engineering*, Vol. 60, No. 6, pp.1636–1644.

Guizzo, E. and Goldstein, H. (2005) 'The rise of the body bots [robotic exoskeletons', *IEEE Spectr*., Vol. 42, No. 10, pp.50–56.

He, H., Kiguchi, K. and Horikawa, E. (2007) 'A study on lower-limb muscle activities during daily lower-limb motions', *International Journal of Bioelectromagnetism*, Vol. 9, No. 2, pp.79–84.

Hofmann, M., Danhard, M. and Betzler, N. (2006) 'Modelling with BRG.LifeMOD®™ in sport science', *International Journal Comp. Sci. Sport*, Vol. 5, pp.68–71.

Hong, Y.W., King, Y-J., Yeo, W-H., Ting, C-H., Chuah, Y-D., Lee, J-V. and Chok, E-T. (2013) 'Lower extremity exoskeleton: review and challenges surrounding the technology and its role in rehabilitation of lower limbs', *Australian Journal of Basic and Applied Sciences*, Vol. 7, No. 7, pp.520–524.

Hussain, S., Xie, S.Q. and Jamwal, P.K. (2013a) 'Control of a robotic orhtosis for gait rehabilitation', *Robotics and Autonomous Systems*, Vol. 61, No. 9, pp.911–919.

Hussain, S., Xie, S.Q. and Jamwal, P.K. (2013b) 'Effect of cadence regulation on muscle activation patterns during robot assisted gait: a dynamic simulation study', *IEEE Journal of Biomedical and Health Informatics*, Vol. 17, No. 2, pp.442–451.

Kazerooni, H., Chu, A. and Zoss, A. (2005) 'On the biomimetic design of the Berkeley lower extremity exoskeleton (BLEEX)', *IEEE ICRA*, Barcelona, Spain, 18–22 April, pp.4345–4352.

Kim, J-H., Han, J.W., Kim, D.Y. and Baek, Y.S. (2013) 'Design of a walking assistance lower limb exoskeleton for paraplegic patients and hardware validation using CoP', *International Journal of Advanced Robotic Systems*, Vol. 10, pp.113–121.

Li, N., Yan, L., Qian, H., Wu, H., Wu, J. and Men, S. (2015) 'Review on lower extremity exoskeleton robot', *The Open Automation and Control Systems Journal*, Vol. 7, No. 1, pp.441–453.

Lingaiah, K. (2006) *Design Data Hand Book*, Suma Publication, Bangalore, India.

Lundin, T., Grabiner, M. and Jahnigen, D. (1995) 'On the assumption of bilateral lower extremity joint moment symmetry during the sit-to-stand tasks', *Journal of Biomechanics*, Vol. 28, No. 1, pp.109–112.

Mayagoitia, R.E., Nene, A.V. and Veltink, P.H. (2002) 'Accelerometer and rate gyroscope measurement of kinematics: an inexpensive alternative to optical motion analysis systems', *Journal of Biomechanics*, Vol. 35, No. 4, pp.537–542.

Music, J., Kamnik, R. and Munih, M. (2008) 'Model based inertial sensing of human body motion kinematics in sit-to-stand movement', *Simulation Modelling Practice and Theory*, Vol. 16, No. 8, pp.933–944.

Nolte, K., Krüger, P.E., Els, P.S. and Nolte, H.W. (2013) 'Three-dimensional musculoskeletal modelling of the seated row resistance-training exercise', *South African Journal of Sports Medicine*, Vol. 25, No. 3, pp.67–73.

Onen, U., Botsalı, F.M., Kalyoncu, M., Tınkır, M., Yılmaz, N. and Sahin, Y. (2013) 'Design and actuator selection of a lower extremity exoskeleton', *IEEE/ASME Transactions on Mechatronics*.

Rahman, M.H., Kittel-Ouimet, T., Saad, M., Kenn, J.P. and Archambault, P.S. (2011) 'Robot assisted rehabilitation for elbow and forearm movements', *International Journal of Biomechatronics and Biomedical Robotics*, Vol. 1, No. 4, pp.206–218.

Tsukahara, A., Kawanishi, R., Hasegawa, Y. and Sankai, Y. (2010) 'Sit-to-stand and stand-to-sit transfer support for complete paraplegic patients with robot suit HAL', *Advanced Robotics*, Vol. 24, No. 11, pp.1615–1638.

Wang, S., van Dijk, W. and van der Kooij, H. (2011) 'Spring uses in exoskeleton actuation design', *IEEE International Conference on Rehabilitation Robotics*.

Zhang, Y. and Anderson, S. (2012) 'Investigation of energy expenditure for exoskeleton walking: a case study', *International Journal of Biomechatronics and Biomedical Robotics*, Vol. 2, No. 1, pp.26–31.

Zhu, R. and Zhou, Z. (2004) 'A real-time articulated human motion tracking using triaxis inertial/magnetic sensors package', *IEEE Trans. Neural Syst. Rehabil. Eng*., Vol. 12, No. 2, pp.295–302.

Zhu, Y., Zhang, G., Zhang, C., Liu, G. and Zhao, J. (2015) 'Biomechanical modeling and load-carrying simulation of lower limb exoskeleton', *Bio-Medical Materials and Engineering*, Vol. 26, No. s1, pp.729–738.

Zoss, A. and Kazerooni, H. (2005), 'Architecture and hydraulics of a lower extremity exoskeleton', *ASME International Mechanical Engineering Congress and Exposition*.

Zoss, A., Kazerooni, H. and Chu, A. (2005) 'On the mechanical design of the berkeley lower extremity exoskeleton (BLEEX)', *International Conference on Intelligent Robots and Systems*, Vol. 5, pp.3132–3139.